Available online at www.sciencedirect.com
ScienceDirect
Journal of Power Sources 171 (2007) 433–440
JOURNAL OF POWER SOURCES
www.elsevier.com/locate/jpowsour

Cathode structure optimization for air-breathing DMFC by application of pore-forming agents

Tatyana V. Reshetenko, Hee-Tak Kim*, Ho-Jin Kweon

Samsung SDI Co., Ltd., 575 Shin-dong, Yeongtong-gu, Suwon-si, Gyeonggi-do 443-391, Republic of Korea

Received 8 March 2007; accepted 14 May 2007
Available online 21 June 2007

Abstract

The cathode catalyst layer in an air-breathing, direct methanol fuel cell (DMFC) has been improved by addition of pore-forming materials, such as ammonium carbonate and ammonium hydrocarbonate. These construct an effective electrode pore structure. During fabrication of the membrane electrode assembly (MEA), these pore-formers decompose, increase the BET surface area of the electrodes, and form additional porosity. Ammonium carbonate predominantly produces macropores, while ammonium hydrocarbonate is effective for mesopores. This results in an increase in electrochemical active area and catalyst utilization. The higher open-circuit voltage with MEAs prepared with pore-forming material indicates improved air transfer through the cathode. The power density is increased by 30–40% with the employment of the pore-forming materials.

Keywords: Direct methanol fuel cell; Air-breathing; Pore-forming material; Membrane electrode assembly; Power density; Catalyst utilization

1. Introduction

Direct methanol fuel cells (DMFCs) are considered as candidates for power sources for mobile application due to their low operating temperature and suitable power density [1–3]. The performance of DMFCs is greatly affected by the properties of the membrane electrode assembly (MEA), which usually consists of a proton-conductive membrane, an anode and a cathode. Each electrode contains an active catalyst layer and a gas-diffusion layer, which provides good electrical contact, mechanical support, and transport of fuel and air. Great efforts have been made in the research of electrochemically active anode/cathode catalysts [4–7] and the development of new membranes [8–10] to improve MEA performance.

There are a number of catalysts layer properties that have to be optimized to achieve high utilization of the catalyst material. For example, catalyst loading, ionomer content, and ionic and electrical conductivity have been receiving attention [11–19]. It is well known, that addition of Nafion (a proton-conductive ionomer) into the catalyst layer enhances fuel cell performance due to increased proton transfer through the catalyst layer and increased catalyst utilization. On the other hand, the structure and morphology of the electrode can affect the mass-transfer of reactants and products, and thereby govern reaction rates. It should be noted that mass-transfer processes, which contribute to performance loss, especially at high current densities, become important in the case of an air-breathing DMFC.

Fuel cells which use one or both reactants by diffusion have great promise due to avoidance of the need for additional equipment (pumps, compressors). They are ideally suited to low-power applications [20–22]. Fuel cells in which both the fuel and the oxidant are supplied by diffusion are known as ‘passive’, and those which take in only one reactant by force convection as ‘semi-passive’. ‘Air-breathing’ fuel cells have an open cathode structure through which air is delivered by means of diffusion. The cathode structure must allow oxygen to reach the catalyst surface and support efficient transport of water to prevent flooding of the catalyst layer, since the catalytic activity of oxygen reduction decreases when the rate of water removal is less than rate of water production. Therefore, the structure and composition of the electrodes, together with electrocatalyst properties, strongly affect the performance of the air-breathing DMFC. The electrode morphology and porous structure can be optimized by fabrication methods [23–26] and by the addition

* Corresponding author. Tel.: +82 31 210 7047; fax: +82 31 210 7374.
E-mail address: hee-tak.kim@samsung.com (H.-T. Kim).

0378-7753/$ – see front matter © 2007 Elsevier B.V. All rights reserved.
doi:10.1016/j.jpowsour.2007.05.105

of pore-forming (PF) agents [27–34]. The application of PF agents of low-temperature decomposable inorganic substances (ammonium carbonate, lithium carbonate, ammonium oxalate) for modification of the electrode structure has been reported for proton exchange membrane fuel cells (PEMFCs) [27–32], and active-type DMFCs [33,34].

It was found [29] that the application of ammonium carbonate to the Pt black cathode layer of a MEA in a high-temperature PEMFC enhanced the catalyst activity and minimized mass-transport limitations. The maximum performance was observed for fuel cell with 20 wt.% $(NH_4)_2CO_3$ and an increase in cell voltage of 19% was reported. Fischer and co-authors [30] disclosed a method for preparation of gas-diffusion electrodes with a PF agent for PEMFCs. Additional coarse porosity was observed by the introduction of pore-forming substances (Li_2CO_3 and $(NH_4)_2CO_3$) to the electrocatalyst slurry. That allowed for better access of oxygen from air to the inside of the cathode and the performance of the fuel cell was enhanced. Gamburzev and Appleby [32] demonstrated improvement in PEMFC performance by the addition of PF material into the electrode. It was shown that the current density at 0.7 V increased from 200 to 600 mA cm^{-2} at 50 °C. Wei et al. [33] found that addition of ammonium oxalate into electrodes resulted in a 30% increase in the power density of an active DMFC at 0.4 V and 75 °C. Improvement in the anode performance of active DMFC has also been achieved [34] by introduction of 50 wt.% Li_2CO_3. Lithium carbonate was added to a Pt-Ru black catalyst ink and was removed after printing of the electrode by washing in 1 M H_2SO_4. It was established that the modified anode had a higher porosity than an anode without PF. Also, the modified MEA showed a significant increase (up to 50%) in power density.

In this study, the cathode pore structure of the MEA in an air-breathing DMFC has been enhanced by using ammonium carbonate (AC) and ammonium hydrocarbonate (AH) as PFs to improve power performance. With varying the content and type of PF, the structural and textural properties of the cathode catalyst layer is investigated by means of scanning electron microscopy (SEM), BET, and mercury porosimetry. The influence of the resulting electrode texture on the electrochemical properties is discussed in terms of current–voltage behaviour and impedance analysis.

2. Experimental

2.1. MEA preparation and characterization

All MEAs were prepared with Nafion 115 (DuPont). The catalysts used, in this work, were Pt-Ru (1:1) black (HiSpec 6000, Johnson Matthey) and Pt black (HiSpec 1000, Johnson Matthey) for the anode and the cathode, respectively. As a diffusion layer, 31 BA (SGL, Germany) was used for the cathode and 31 BC (SGL) for the anode. Catalyst inks, consisting of appropriate amounts of unsupported catalysts, Nafion solution, pore forming agents - AC or AH (Sigma–Aldrich) and isopropyl alcohol were homogenized to disperse the components. The weight ratio of ionomer to catalyst was 0.12 and the weight ratio of PF material to catalyst was varied in the range of 0.03–0.2. To prepare the electrodes, the catalyst ink was sprayed onto the membrane to form a catalyst-coated membrane (CCM). MEAs were obtained by hot pressing at 135 °C and at 51 MPa. The cell active area was 10 cm^2. The loading levels of the catalyst and the pore former are listed in Table 1.

Table 1
Characterization of MEAs (AC - ammonium carbonate, AH - ammonium hydrocarbonate)

Sample	Anode Pt-Ru (mg cm^{-2})	Cathode	
		Pt (mg cm^{-2})	PF/Catalyst ratio
Reference	6.2	7.6	–
AC-0.03	7.5	7.3	0.03
AC-0.05	6.4	6.2	0.05
AC-0.1	6.0	7.6	0.1
AC-0.2	6.5	6.0	0.2
AH-0.03	6.4	6.5	0.03
AH-0.05	6.2	6.7	0.05
AH-0.1	6.2	6.6	0.1
AH-0.2	6.6	6.6	0.2

The morphological characteristics of the catalyst layers were investigated by SEM using a JEOL JSM-6700F microscope. The particle-size distribution of the catalyst ink was measured with an ELS-800 instrument (Photal Otsuka Electronics). Adsorption measurements were carried out using an ASAP 2020 instrument (Micromeritics) with adsorption of nitrogen at 77 K. The adsorption isotherms were used to calculate the surface area (A_{BET}), mesopore volume (V_{meso}), and pore-size distribution. The porosity of the electrodes was also determined using a mercury porosimetry (MP) with an AutoPore IV (Micromeritics) and total pore volume was measured (V_{total}).

2.2. Electrochemical analysis

Polarization curves were recorded using a MEA test station (Fuel Cell Technologies Inc.). The MEAs were sandwiched between an anode monopolar plate with serpentine flow channels and a cathode-current collector with holes. Electrical heaters and a thermocouple were embedded in the plates for controlling the desired operating temperature. An aqueous methanol solution was delivered to the anode compartment by a pump.

As a pre-conditioning step, *I–V* polarization curves were measured at 1 M CH_3OH and 50 °C (anode stoichiometry = 3) for five times. Then, the solution was replaced by 3 M CH_3OH (anode stoichiometry = 2) and the final polarization curves were obtained. It should be noted that at current densities below 100 mA cm^{-2}, the methanol flow rate was set constant (0.069 ml min^{-1}). The cell temperature was varied in the range 50–70 °C.

Electrochemical impedance spectra (EIS) were recorded using a MEA test station (Fuel Cell Technologies Inc.), in which a frequency response analyzer is installed, at 50 °C in the frequency range from 100 kHz to 100 mHz. Impedances were measured under galvanostatic control of the cell. The amplitude of the sinusoidal voltage signal did not exceed 10 mV.

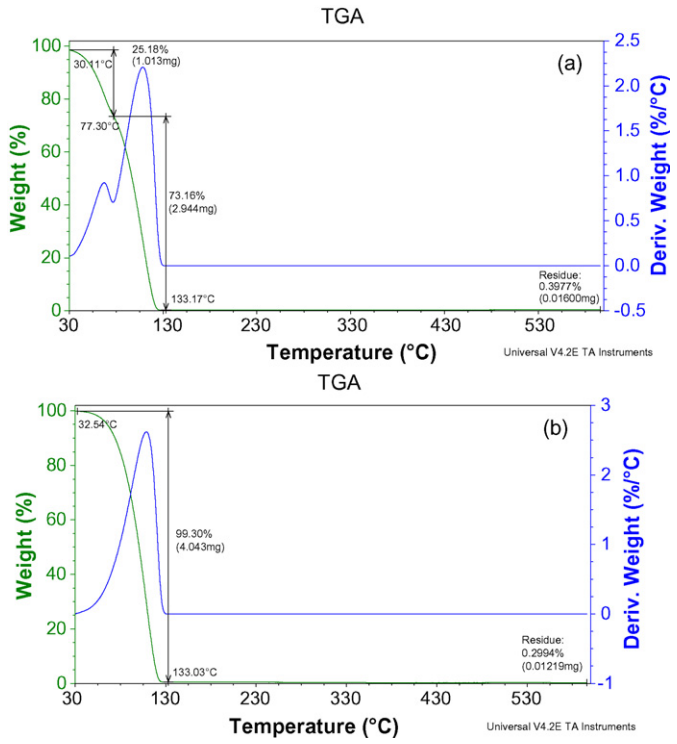

Fig. 1. Thermogravimetric analysis of applied pore-forming agents: (a) $(NH_4)_2CO_3$ and (b) NH_4HCO_3.

3. Results and discussions

3.1. Characterization of PF agents

AC and AH were chosen as the pore-forming agents since they can completely decompose to NH_3, CO_2 and water at relatively low-temperatures. Fig. 1(a and b) shows the thermogravimetric analysis (TGA) of these compounds from room temperature to 600 °C at heating rate of 10° min^{-1} in air. These compounds start to decompose at 70–80 °C, and they are finally destroyed at 130 °C. So heat-treatment of the electrode with AC or AH at 135 °C allows these compounds to decompose. It was known that Nafion membrane is chemically stable at that temperature [29].

Fig. 2(a and b) presents optical microscopic images of AC and AH crystals. The crystal size is in the range of 30–50 μm. These are insoluble in isopropyl alcohol, and can be broken into smaller particle during the homogenization of the slurry. At the same time, the cathode slurry has a Pt particle-size distribution with a maximum height at 200–300 nm (Fig. 3). So, addition of ammonium carbonate and hydrocarbonate should cause the formation of coarse pores, and a modification of the textural properties can be expected.

3.2. Electrode morphology

Scanning electron micrographs (Fig. 4) illustrate the morphology of the cathodes under the study. The micrographs allow coarse or macropores (0.5–1 μm) and fine or mesopores (below 0.1 μm) to be distinguished in the electrodes prepared with the

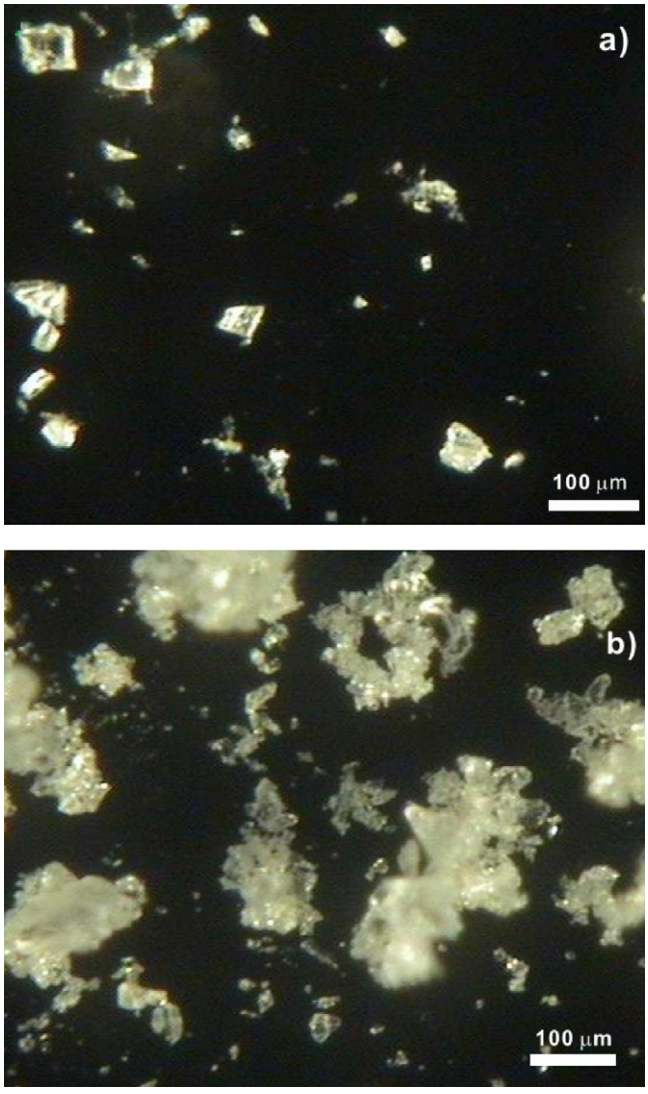

Fig. 2. Optical images of pore-formers: (a) $(NH_4)_2CO_3$ and (b) NH_4HCO_3.

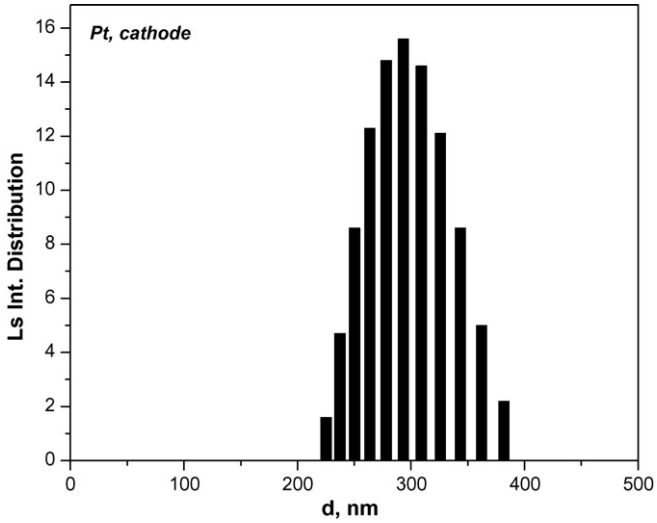

Fig. 3. Pt particle-size distribution of cathode catalyst ink.

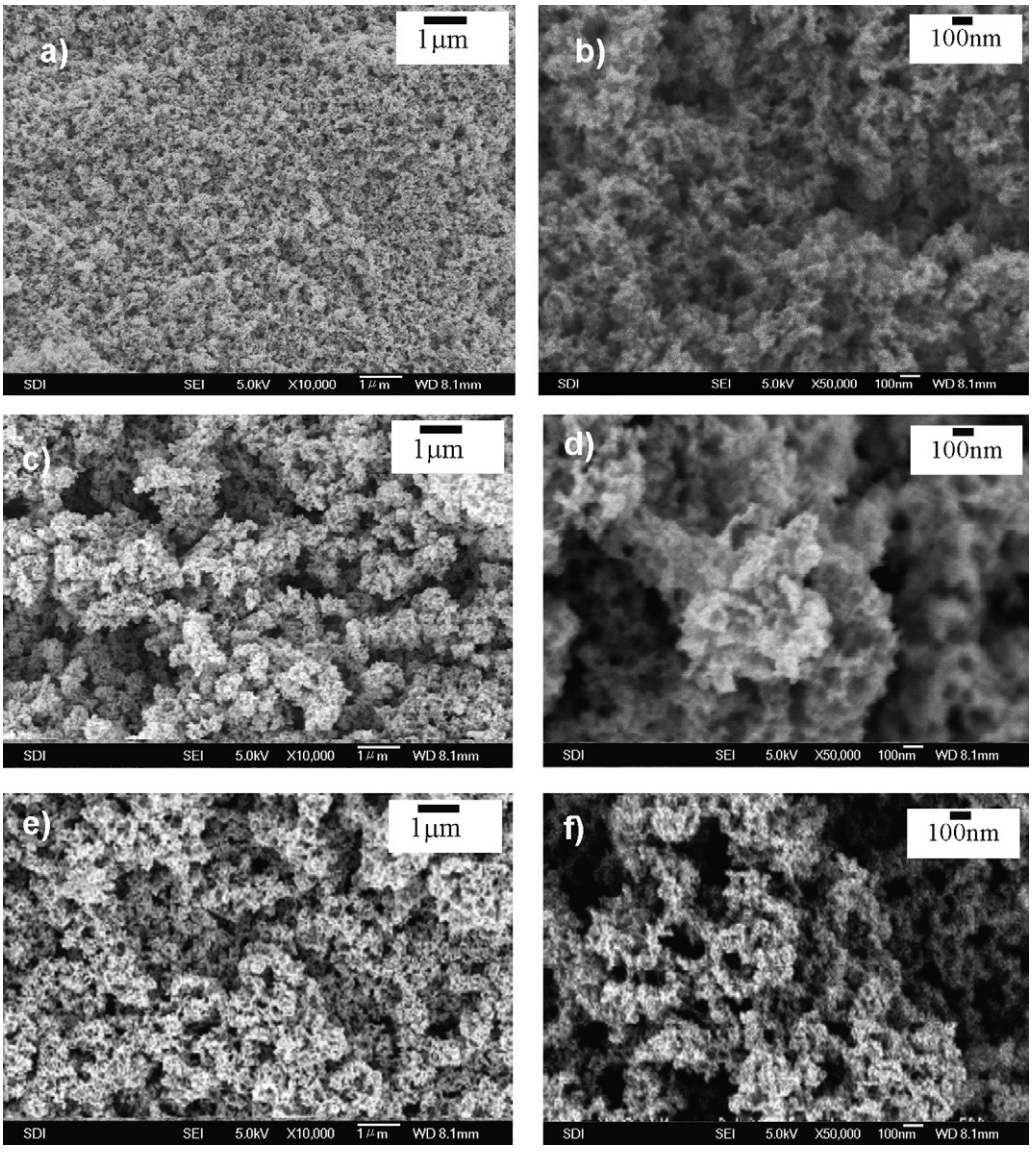

Fig. 4. Scanning electron micrographs of cathodes under study: (a and b) reference; (c and d) AC-0.05; (e and f) AH-0.05.

PF agents. By contrast, the electrode prepared without the PF agent did not reveal large amount of the coarse pores, which indicates that the coarse pores in the modified cathodes are attributed to the PF agents.

In order to determine the effect of the PF agents on the mesoporous structure of the catalyst layer, the pore-size distribution was measured by BET. As shown in Fig. 5a, the mesopore-size distribution is not changed significantly in AC samples. The pore-size distribution of the AH cathodes (Fig. 5b) shows a shift of the distribution maximum, namely, the reference electrode (no AH) has the maximum at 20–30 nm, but the maximum for the modified electrodes is 60–70 nm. Table 2 clearly shows that there is an increase in the mesopore volume (V_{meso}) with PF loading for both AC and AH series. The AH sample exhibits more significant volume growth than the AC counterpart. Also, an increase in BET surface area is shown by the modified cathodes.

The total pore volume (V_{total}) was calculated from a mercury intrusion curve and includes pores from 10 nm to 300 μm (meso and macropores) (Table 2). The AC samples experience a significant increase in the total pore volume while a smaller growth of V_{total} is observed for the AH series. Comparison of the meso and total pore volumes shows that ammonium carbonate promotes mainly the formation of macropores, while ammonium hydro-

Table 2
Textural properties of cathodes

Sample	A_{BET} ($m^2\ g^{-1}$)	V_{meso} ($cm^3\ g^{-1}$)	V_{total} ($cm^3\ g^{-1}$)
Reference	1.66	0.012	0.238
AC-0.03	3.32	0.013	–
AC-0.05	3.52	0.017	0.292
AC-0.1	3.20	0.014	0.297
AC-0.2	3.57	0.015	0.289
AH-0.03	3.16	0.027	–
AH-0.05	4.32	0.035	0.279
AH-0.1	3.84	0.032	0.264
AH-0.2	5.06	0.040	0.252

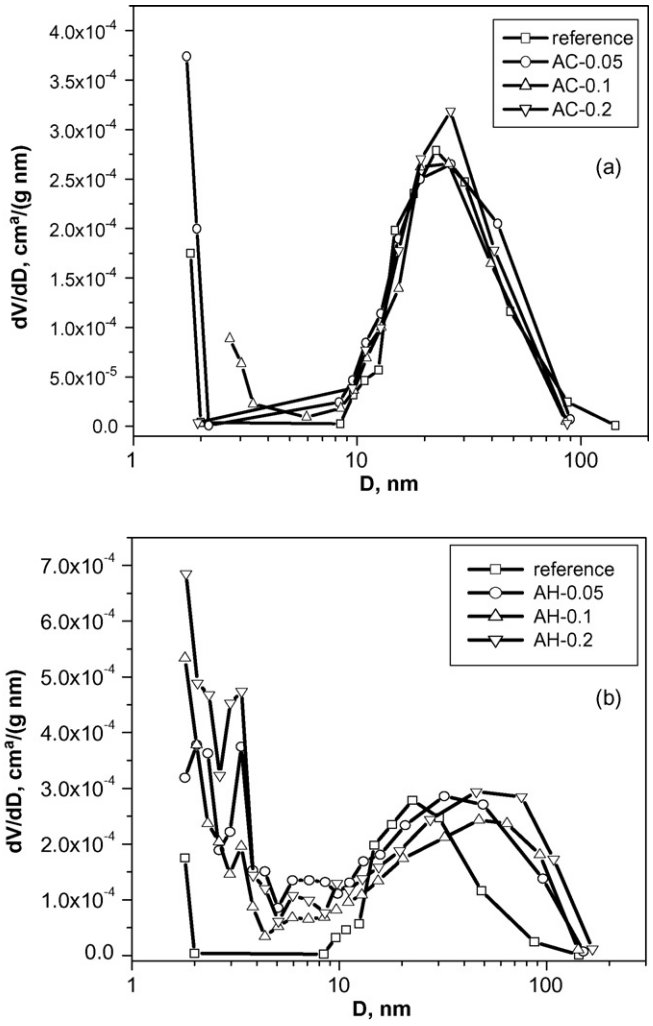

Fig. 5. Pore-size distribution of cathodes determined by BET: (a) electrodes modified by $(NH_4)_2CO_3$ and (b) electrodes modified by NH_4HCO_3.

carbonate is effective for mesopores. This behaviour appears to originate from a difference in the crystal size of the PF agents (Fig. 2).

3.3. MEA performance and impedance spectra

Table 3 summarizes the influence of the PF loading on the power density of the MEAs. A maximum performance was usually observed on the fourth day of the evaluation. Such an activation effect may be considered to arise from time-dependent hydration of the electrode layers, which cause structural changes in the catalysts [35,36]. As can be seen, introduction of AC and AH (PF ratio of 0.03–0.1) leads to an increase in power density. Nonetheless, there is a decrease of performance with further increase in AH loading; the MEA with a AH ratio of 0.2 gives inferior activity, suggesting that there exists an optimum loading of the pore former.

The effect of PF additives on the polarization characteristics of the studied MEAs is shown in Fig. 6(a and b). All samples except AH-0.2 demonstrate an improvement in performance in both the low- and high-current density regions. Enhancement of the performance at low-current densities may be explained by a higher degree of catalyst utilization and an increase in the electrochemical active area [29,30]. The change in the catalyst utilization might be identified by the *I–V* curves at current densities of 0–0.1 mA cm^{-2}. In this region, the performance of the DMFC is controlled mainly by electrode kinetics, which is directly related to the total amount of the reactant–catalyst–electrolyte sites [37]. The inset in Fig. 6(a and b) illustrates that the current densities at the same voltage increase for the modified MEAs. Since the catalyst loading is nearly the same for all the MEAs, the observed increase in the current density results from an increase in catalyst utilization.

Fig. 7 presents the EIS curves recorded at a current density of 150 mA cm^{-2} where electrode kinetics govern the electrochemical process. Each curve has two semi-circles. The low-frequency loop is attributed to the anode reaction, and the high frequency to the cathode reaction. Since the kinetics of methanol electrooxidation are much slower than those of oxygen reduction, the impedance associated with methanol oxidation should be revealed at lower frequency. The anode loops for all studied MEAs are close, which may be explained by little difference

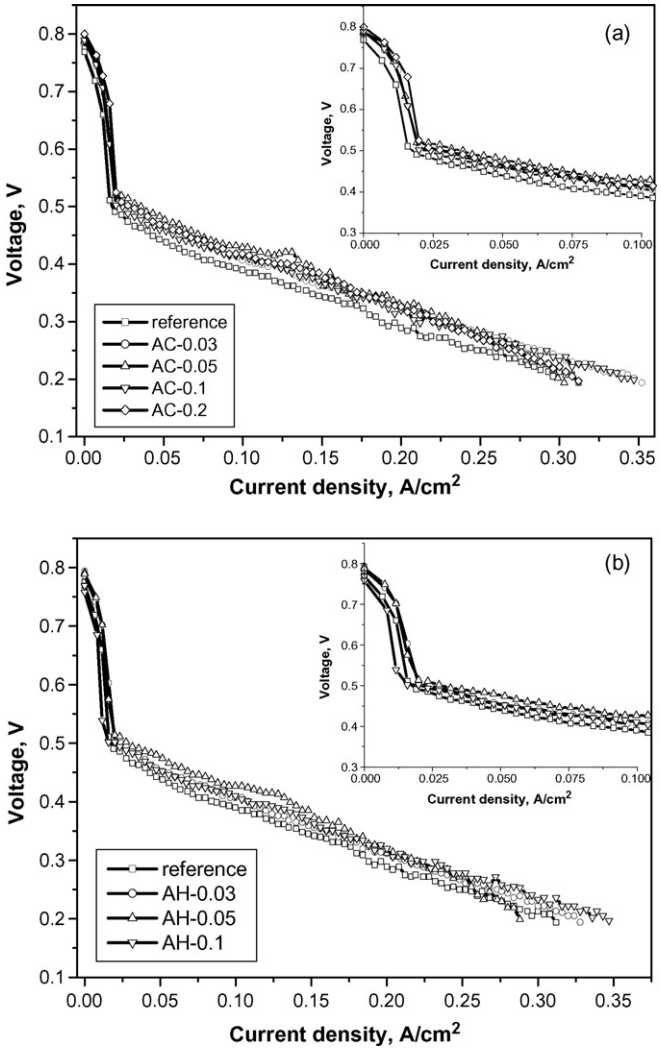

Fig. 6. Polarization curves for samples modified by: (a) $(NH_4)_2CO_3$ and (b) NH_4HCO_3 ($T = 50\,^{\circ}C$, 3 M MeOH, 4 day of evaluation).

Table 3
Power densities of samples under the study

Sample	OCV, V (50 °C)	T (°C)	Power density at 0.33 V (mW cm^{-2})								
			1 day	2 day	3 day	4 day	5 day	6 day	7 day	8 day	9 day
Reference	0.775	50	24	42	50	52	55	54	36		
		70	45	64	70	70	71	73	43		
AC-0.03	0.786	50	20	39	50	65	54	60	61	64	58
		70	35	67	76	83	77	80	66	71	72
AC-0.05	0.786	50	26	53	63	69	70	65			
		70	47	71	90	84	85	57			
AC-0.1	0.797	50	12	42	54	62	68	66	60		
		70	21	61	77	92	93	91	84		
AC-0.2	0.800	50	10	31	49	64	64	65	63	54	
		70	16	52	73	85	85	85	85	79	
AH-0.03	0.794	15	34	54	60	54	60	60	56		
		27	64	64	74	60	75	75	70		
AH-0.05	0.791	50	20	44	58	62	60	63	70	86	
		70	34	58	75	77	80	91	93	69	
AH-0.1	0.770	50	15	48	60	64	72	73	70	70	58
		70	26	73	89	98	92	90	87	87	78
AH-0.2	–	50	4	7							
		70	4	8							

in the anode structure and composition between these MEAs. By contrast, differences can be distinguished for the cathode semi-circles. Introduction of AC or AH results in a smaller cathode semi-circle in comparison with the reference sample, which indicates faster electrochemical reduction.

In the present study, the same cathode catalyst was used. Therefore, the intrinsic activity of catalyst is expected to be the same for all MEAs. The observed differences can be explained in terms of extension of the gas–electrolyte–catalyst surface and reduction of mass-transfer limitations. Earlier, it was shown that the electrode layer consists of catalyst agglomerates, which contain the primary catalyst particles. Usually, these agglomerates are coated by Nafion film to provide a three-dimensional reaction zone [38]. This suggests that primary Pt particles loaded inside the agglomerates do not take part in the reactions, since they are out of contact with the polymer electrolyte. Also, the regions could be blocked or enclosed so that gaseous reactant cannot access these 'dead' zones. The addition of pore formers appears to open the regions and make them active, and to expand the three-phase boundary. Therefore, an increase in pore volume is likely to improve the electrochemical active area and reduce cathode impedance. The results also indicate a reduction in the mass-transfer limitation in the cathode electrode. Increased pore volume is expected to enhance mass-transfer near the catalyst surface by providing open diffusion paths for produced water from the electrode and facilitating faster oxygen supply inside the catalyst layer.

On the other hand, it is interesting to note that open-circuit voltage (OCV) is increased with the addition of PF agents, as can be seen in Fig. 6 and Table 3. Since any methanol that crosses over the membrane from the anode to cathode will react with oxygen, oxygen depletion at the cathode near the membrane is expected. A low oxygen concentration will result in a decrease of the cathode potential, which will lead to lowering of the OCV. In the case of fast supply of oxygen through the cathode catalyst layer, the concentration in the cathode will be enhanced and the OCV is expected to be higher. The macro pores generated by PF agents may act as an effective channel for air transport. The charge-transfer reaction is also a function of reactant concentration. An enhanced oxygen supply accelerates the oxygen reduction reaction.

The low-performance of the AH-0.2 samples is likely related to a decrease in the effective ionic conductivity due to high-porosity and a restricted three-phase boundary. The effective ionic conductivity of the catalyst layer ($\sigma_{H+,eff}$) is a function of the Nafion volume fraction (ε), the conductivity of the Nafion (σ_{Nafion}) and the tortuosity of the proton paths in the electrode (n) [39], i.e.,

$$\sigma_{H+,eff} = \sigma_{Nafion}\varepsilon^{n} \quad (1)$$

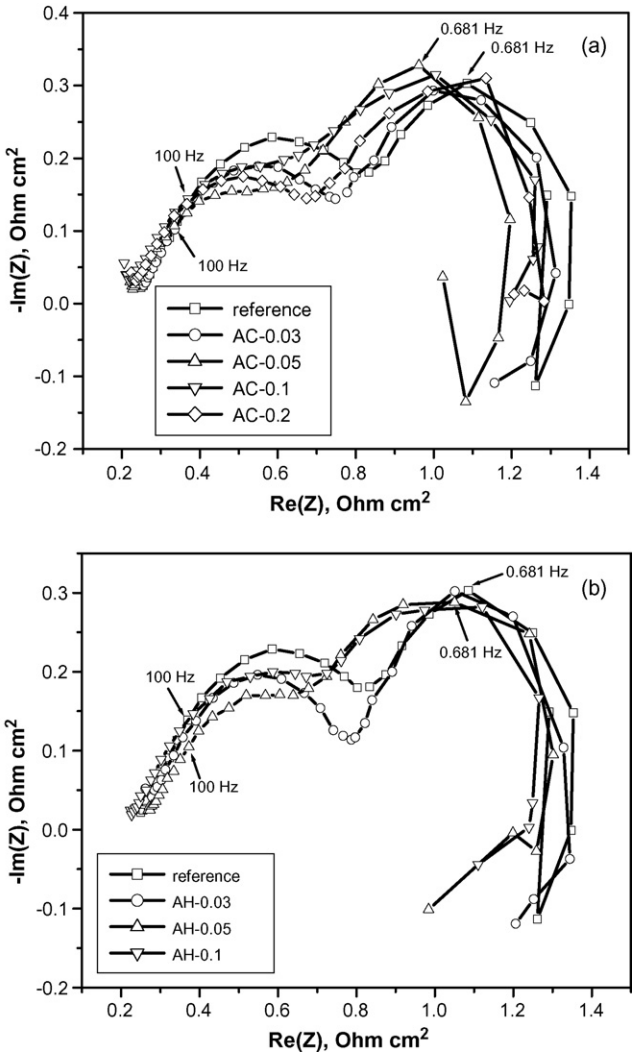

Fig. 7. EIS curves for DMFC: (a) $(NH_4)_2CO_3$ and (b) NH_4HCO_3 ($T = 50\,^{\circ}C$, 3 M MeOH, 4 day of evaluation, $i = 150\,mA\,cm^{-2}$).

According to this equation, an increase in the amount of PF agent in the electrode leads to a decrease of the Nafion fraction, which results in a loss of effective ionic conductivity and active gas–electrolyte–catalyst surface, and thereby, a fall in cell performance is observed. Optimization of the Nafion content in the electrode layer, in this case, might improve MEA performance.

4. Conclusions

Introduction of pore-forming materials, such as AC and AH and optimization of their loadings improves the performance of DMFCs operating under air-breathing conditions. It is found that addition of AC (AC/catalyst = 0.05) or AH (AH/catalyst = 0.05–0.1) increases the power density up to 70–75 mW cm^{-2} at 50 °C. Further increase in the AC/catalayst ratio to 0.2 causes a reduction in the cell performance, which is probably due to the loss of effective ionic conductivity and a reduced gas–electrolyte–catalyst surface.

The PF agents significantly modify the textural properties of the cathodes. It is established that AC mainly promotes the formation of macropores, while the introduction of AH results in an increase in the mesopores volume. It should be noted that an increase in the BET surface area of the cathodes is also observed. Such modification of the electrode texture appears to result in increases in the electrochemical active area and catalyst utilization. Also, the extra-porosity assists oxygen transfer to the catalyst surface, which results in a higher OCV and an improvement in DMFC performance.

References

[1] C.Y. Chen, P. Yang, J. Power Sources 123 (2003) 37.
[2] C. Xie, J. Bostaph, J. Pavio, J. Power Sources 136 (2004) 55.
[3] H. Dohle, H. Schmitz, T. Bewer, J. Mergel, D. Stolten, J. Power Sources 106 (2002) 313.
[4] A.S. Arico, S. Srinivasan, V. Antonucci, Fuel Cells 1 (2001) 133.
[5] M.P. Hogarth, T.R. Ralph, Platinum Met. Rev. 46 (2002) 146.
[6] V. Rao, P.A. Simonov, E.R. Savinova, G.V. Plaksin, S.V. Cherepanova, G.N. Kryukova, U. Stimming, J. Power Sources 145 (2005) 178.
[7] W. Vielstich, A. Lamm, H.A. Gasteiger (Eds.), Handbook of Fuel Cells, 4, John Willey & Sons, 2002.
[8] M. Walker, K.M. Baumgartner, M. Kaiser, J. Kerres, A. Ullrich, E. Rauchle, J. Appl. Polymer Sci. 74 (1999) 67.
[9] J.A. Kerres, J. Membrane Sci. 185 (2001) 3.
[10] V. Baglio, A.S. Arico, A. DiBlasi, V. Antonucci, P.L. Antonucci, S. Licoccia, E. Traversa, F. Serraino Fiory, Electrochem. Acta 50 (2005) 1241.
[11] D. Song, Q. Wang, Z. Liu, M. Eikerling, Z. Xie, T. Navessin, S. Holdcroft, Electrochem. Acta 50 (2005) 3347.
[12] S. Wang, G. Sun, G. Wang, Z. Zhou, X. Zhao, H. Sun, X. Fan, B. Yi, Q. Xin, Electrochem. Commun. 7 (2005) 1007.
[13] V. Gogel, T. Frey, Z. Yongsheng, K.A. Friedrich, L. Jorissen, J. Garche, J. Power Sources 127 (2004) 172.
[14] S.Q. Song, Z.X. Liang, W.J. Zhou, G.Q. Sun, Q. Xin, V. Stergiopoulos, P. Tsiakaras, J. Power Sources 145 (2005) 495.
[15] N. Nakagawa, Y. Xiu, J. Power Sources 118 (2003) 248.
[16] L. Liu, C. Pu, R. Viswanathan, Q. Fan, R. Liu, E.S. Smotkin, Electrochem. Acta 43 (1998) 3657.
[17] K. Furukawa, K. Okajima, M. Sudoh, J. Power Sources 139 (2005) 9.
[18] S.C. Thomas, X. Ren, S. Gottesfeld, J. Electrochem. Soc. 146 (1999) 4354.
[19] T.V. Reshetenko, H.-T. Kim, H. Lee, M. Jang, H.-J. Kweon, J. Power Sources 160 (2006) 925.
[20] J.G. Liu, T.S. Zhao, R. Chen, C.W. Wong, Electrochem. Commun. 7 (2005) 288.
[21] Y.H. Pan, J. Power Sources 161 (2006) 282.
[22] B.P.M. Rajani, A.K. Kolar, J. Power Sources 164 (2007) 210.
[23] M.S. Wilson, J.A. Valerio, S. Gottesfeld, Electrochim. Acta 40 (1995) 355.
[24] M. Uchida, Y. Fukuoka, Y. Sugawara, H. Ohara, A. Ohta, J. Electrochem. Soc. 145 (1998) 3708.
[25] X. Cheng, B. Yi, M. Han, J. Zhang, Y. Qiao, J. Yu, J. Power Sources 79 (1999) 75.
[26] C.Y. Chen, C.S. Tsao, Int. J. Hydrogen Energ. 31 (2006) 391.
[27] Y.-G. Yoon, G.-G. Park, T.-H. Yang, J.-H. Han, W.-Y. Lee, C.-S. Kim, Int. J. Hydrogen Energ. 28 (2003) 657.
[28] M. Chisaka, H. Daiguji, Electrochem. Acta 51 (2006) 4828.
[29] Y. Song, Y. Wei, H. Xu, M. Williams, Y. Liu, L.J. Bonville, H.R. Kunz, J.M. Fenton, J. Power Sources 141 (2005) 250.
[30] A. Fischer, J. Jindra, H. Wendt, J. Appl. Electrochem. 28 (1998) 277.
[31] K. Fukuda, I. Tanaka, M. Tani, J. Matsuo, EP Patent 1,429,403.
[32] S. Gamburzev, A.J. Appleby, J. Power Sources 107 (2002) 5.
[33] Z. Wei, S. Wang, B. Yi, J. Liu, L. Chen, W. Zhou, W. Li, Q. Xin, J. Power Sources 106 (2002) 364.

[34] M.C. Tucker, M. Odgaard, P.B. Lund, S. Yde-Andersen, J.O. Thomas, J. Electrochem. Soc. 152 (2005) A1844.
[35] C. Lim, C.Y. Wang, J. Power Sources 113 (2003) 145.
[36] B.-K. Kho, I.-H. Oh, S.-A. Hong, H.-Y. Ha, Electrocem. Acta 50 (2004) 781.
[37] C. He, Z. Qi, M. Hollett, A. Kaufman, Electrochem. Solid-State Lett. 5 (2002) A181.
[38] M. Uchida, Y. Fukuoka, Y. Sugawara, N. Eda, A. Ohta, J. Electrochem. Soc. 143 (1996) 2245.
[39] A. Havranek, K. Wippermann, J. Electroanal. Chem. 567 (2004) 305.